

## Porous InP as Piezoelectric Component in Magnetolectric Composite Sensors

M.-D. Gerngross<sup>a</sup>, V. Sprincean<sup>b</sup>, M. Leisner<sup>a</sup>, J. Carstensen<sup>a</sup>, H. Föll<sup>a</sup>, and I. Tiginyanu<sup>b</sup>

<sup>a</sup> Institute for Materials Science, Christian-Albrechts-University of Kiel, Kaiserstrasse 2,  
24143 Kiel, Germany

<sup>b</sup> Institute of Electronic Engineering and Nanotechnology, Academy of Sciences of  
Moldova, Academy Str. 3/3, Chisinau MD-2028, Moldova

We report on the fabrication of cheap piezoelectric porous InP templates by electrochemical etching and additional purely chemical post-etching and on the galvanic filling of the resulting nanopore array with Ni-Fe using a highly viscous electrolyte.

The  $d_{14}$  component of porous InP is found to be around a stunning  $|60|$  pm/V. The deposited Ni-Fe shows a very narrow hysteresis loop with low coercive field strength (170 G) and very low remanence (0.005 emu).

### Introduction

This paper focuses on the production of an effective and cheap piezoelectric material and on the filling with Ni-Fe for the application in a magnetolectric composite sensor. In this concept porous and piezoelectric InP serves as the matrix material. The pores are then electrochemically filled with a magnetostrictive material. This arrangement of piezoelectric and magnetostrictive materials is chosen, because it allows for very large contact areas, good mechanical coupling between both components, and thus high sensitivity to magnetic fields.

InP, as all III-V semiconductors, is known to show piezoelectric behavior, since InP has no inversion center due to its cubic crystal structure. Thus only the  $d_{14}$  component is a non-vanishing component of the piezoelectric modulus (1). The piezoelectric effect of InP has been measured very rarely (2, 3) because even InP with high purity contains too many impurities as doping centers producing a sufficiently large number of free charge carriers that will short-circuit the charges induced by the piezoelectric effect.

Our approach to overcome the short-circuiting of the polarization induced by the piezoelectric effect is to produce a closed packed pore array with overlapping space charge regions, where no free charge carriers are present.

In the second step, these porous InP structures shall be filled electrochemically with strongly magnetostrictive Ni-Fe/Fe-Ga multilayers. Lupu et al. (4) already demonstrated the electrochemical deposition of Ni-Fe and Fe-Ga in commercially available anodic aluminium oxide (AAO) membranes with pore dimensions comparable to the pore dimensions obtained in InP. This paper focuses also on first results concerning the galvanic filling of the pores with Ni-Fe.

## Experimental

### Pore Etching in InP

The formation of the necessary so-called current-line pores in n-type InP by electrochemical etching is a standard process by now (5). Single crystalline (100) InP wafers doped with S and a doping level  $N_D = 1.1 \cdot 10^{17} \text{ cm}^{-3}$  are used. The resistivity is  $0.019 \Omega\text{cm}$ . The thickness of the wafers is  $500 \mu\text{m} \pm 10 \mu\text{m}$ . The sample size is  $A = 0.25 \text{ cm}^2$ . Experiments have been performed in the electrochemical double-cell described in full detail in (6). As electrolyte, aqueous HCl with a concentration of 6 wt. % has been used. All electrochemical etching experiments have been performed under potentiostatic conditions at a constant temperature of  $T = 20 \text{ }^\circ\text{C}$ . A voltage pulse of 15 V has been applied for 1 s to obtain a homogenous pore nucleation, followed by a constant etching potential of 7 V for 70 min for the samples used for the piezoelectric characterization and 1.5 min for the samples used for galvanic filling.

The etched porous InP nanostructures have been investigated with a HELIOS D477 SEM. The piezoelectric response to an applied voltage has been measured with a double beam laser interferometer (DBLI) from aixACCT.

### Galvanic Filling of the InP Templates

For all filling experiments a three electrode configuration has been used: a Pt counter electrode, a Pt reference electrode, both immersed into the electrolyte, and a Pt working electrode connected to the InP sample. The reference electrode is necessary for the in-situ impedance measurement of the deposition process. These results are not discussed within this paper. The sample is immersed into the electrolyte bath, whose composition is given in Table I. This electrolyte bath is based on the electrolyte of Lupu et al. (4) with some modifications. The addition of carboxymethyl cellulose (CMC) strongly increases the viscosity of the electrolyte. This is necessary to provide a strong diffusion limitation, so that metal deposition onto the sample's surface is prevented. Sodium 2-mercapto-5-benzimidazolesulfonic acid (MBIS) allows for superconformal filling of the porous structures (7). The pH is kept constant at 3.

**TABLE I.** Electrolyte composition for Ni-Fe deposition.

Nickel (II) sulfate	Iron (II) sulfate	Boric acid	Ascorbic acid	Sodium citrate	CMC	MBIS
(g/l)	(g/l)	(g/l)	(g/l)	(g/l)	(g/l)	(mg/l)
218.00	41.72	30.92	1.76	34.28	10	0.29

The electrochemical deposition is always performed at  $20 \text{ }^\circ\text{C}$ . A pulsed current is provided by an ELYPOR-2 potentiostat from ET&TE. A cathodic current of  $-5 \text{ mA}$  is applied to a sample area of  $A = 0.25 \text{ cm}^2$  between counter and working electrode during the pulses. One can only provide a rough estimate of the current density, because the current density has to be given with respect to the pore wall and pore tip area. Taking this into account, the current density is calculated to be around  $0.6 \text{ mA/cm}^2$ . The pulse length is 800 ms. After each pulse a delay time of 4600 ms with 0 mA is applied to replenish the metal ions which are reduced due to the cathodic current pulse. The deposition time is 60

min. This deposition concept is inspired by the concept of Tiginyanu et al. shown in (8) for the electrochemical deposition of Pt in an InP pore array.

The magnetic properties of the electrochemically deposited Ni-Fe coatings are characterized by a vibrating sample magnetometer (VSM) from LakeShore VSM 7300. Before the magnetic characterization in the VSM the deposited Ni-Fe film on the surface is removed by mechanical grinding. The chemical composition is determined by energy dispersive x-ray spectroscopy (EDX).

## Results and Discussion

### Pore Etching in InP

Figure 1 (a) shows the resulting pore structure in top view after electrochemical etching and subsequent removal of the nucleation layer by mechanical polishing. The nucleation layer is only removed for imaging the underlying pore structure with the SEM. The structure is optimized to produce a self-organized pore structure as densely packed as possible. The formation of oxide surface at the pore tips during the electrochemical etching is not a decisive point, because it is well known that the InP oxides easily dissolve in aqueous HCl solutions \cite{KikMat2000}.

The electrochemical etching of current-line pores into bulk InP already reduces the conductivity of the sample in comparison to bulk InP. Porous membranes already show piezoelectric behavior, but the “leakage” currents are still too high for the intended use. This is probably due to some areas where no space charge region is present and thus free charges still short-circuit the induced polarization. These areas without space charge region are due to the non-ideality of the pore geometry and arrangement. To overcome this problem the porous structure from Fig. 1 (a) is chemically post-etched in an HF : HNO<sub>3</sub> : EtOH : HAc solution for 48 h to remove space-charge free areas still left after electrochemical etching (10). This process was optimized to be isotropic and self-limiting; it produces elliptical/circular pore shapes with a mean pore wall thickness of about 150 nm. The resulting pore structure is shown in Fig. 1 (b).

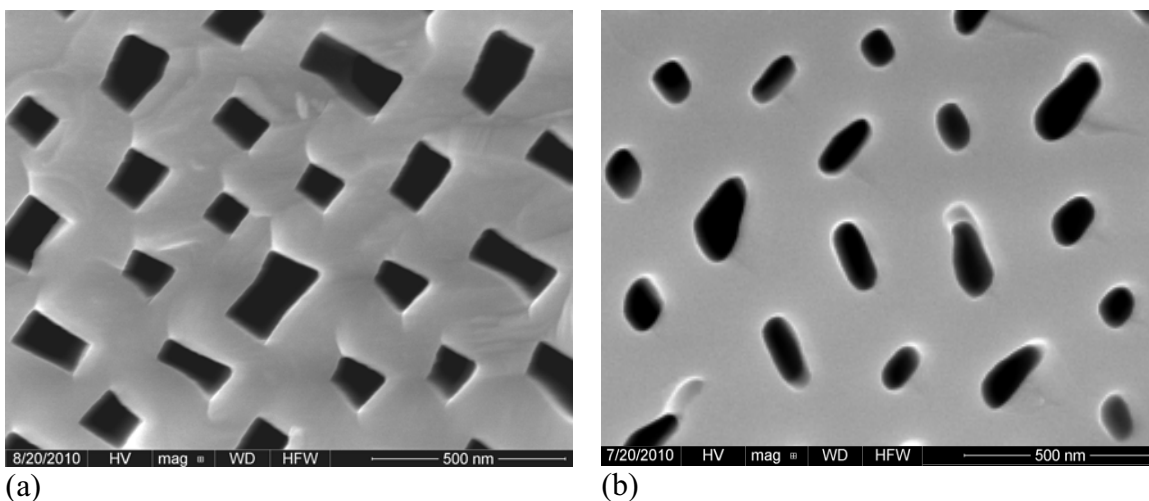


Figure 1. SEM images of n-type InP pore structures after: (a) only electrochemical etching, (b) electrochemical and chemical post-etching.

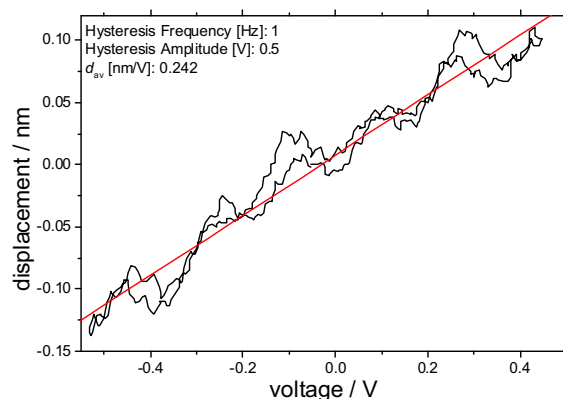


Figure 2. DBLI measurement of the electrochemically and chemically post-etched sample.

The characteristic change in the pore geometry can be understood by considering the space charge region surrounding each pore, the resulting voltage drop across the space charge region and the crystal-orientation dependence of the electrochemical and chemical etching in InP. The pores are expanding in all directions, until an overlap of space charge regions of neighboring pores occurs, which allows no further dissolution of the InP by the post-etchant.

The chemical post-etching of the electrochemically etched samples reduces the leakage currents to a level low enough to use the piezoelectric properties. Figure 2 shows the result of the DBLI measurement of the electrochemically etched and post-etched sample. The DBLI measures the displacement of the InP sample due to the piezoelectric effect as a function of the voltage, which is externally applied in  $\langle 100 \rangle$  direction of the sample via two micromanipulators. The voltage is linearly increased from 0 V to 0.5 V, then linearly decreased to  $-0.5$  V and finally increased to 0 V again. The resulting displacement of the InP sample is measured.

The waviness of the curve is an artifact of specimen mounting. From the slope of the linear displacement vs. applied voltage curve, the  $d_{14}$  component of the porous InP can be derived. It is found to be around  $|60|$  pm/V, about a factor of 30 larger than the values measured on bulk InP (10).

### Galvanic Filling of the InP Templates

Figures 3 (a) and (b) show the result of the electrochemically filling of the pores with Ni-Fe. The nucleation layer of the InP pore array is filled completely with Ni-Fe, while the remaining parts of the pores are only partially filled.

This is due to the fact that the pore diameter reduces from the nucleation layer to the regular hexagonally arranged current line pores, so that after a certain time of galvanic filling the tips of the nucleation layer pores are plugged with Ni-Fe preventing the electrolyte to flow into deeper regions of the regular pores. This can be clearly seen in Fig. 3 (a). Nevertheless the deeper regions show a high level of coverage with Ni-Fe crystallites that are homogeneously distributed over all pores – as shown in Fig. 3 (b).

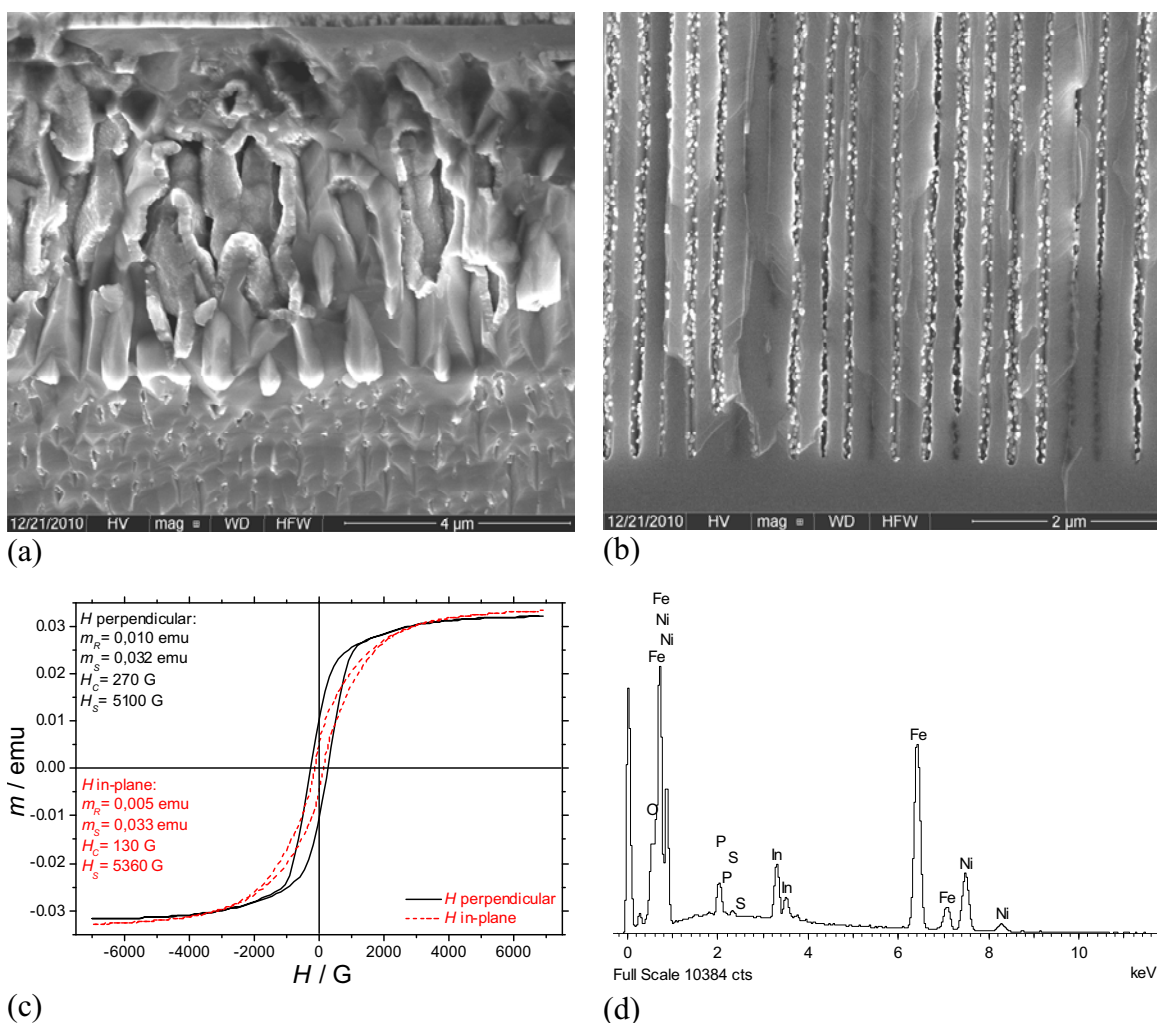


Figure 3. SEM images of n-type InP pore structures after galvanic filling with Ni-Fe: (a) top part (nucleation layer), (b) bottom part of the porous structure, (c) hysteresis loops as a function of the applied magnetic field for the Ni-Fe nanotube array in InP, and (d) EDX spectrum of the Ni-Fe nanotube array in InP.

In Fig. 3 (c) the magnetic properties of the deposited Ni-Fe are shown. Both hysteresis loops for the deposited Ni-Fe are very narrow. The easy magnetization axis of the Ni-Fe nanotubes is in-plane. Here in-plane means parallel to the samples surface, but perpendicular to the Ni-Fe filled pores. The Ni-Fe nanotubes show a very small remanence. The remanence for the easy axis is smaller by a factor of two compared to the hard axis. The nanotubes show a low coercive field strength (130 G for the easy axis). Like the remanence, the coercive field strength is a factor of two smaller for the easy axis compared to the hard axis. The saturation field strength is only slightly lower for the easy axis.

The quantitative analysis of the EDX spectrum from Fig. 3 (d) indicates a composition of  $\text{Ni}_{33}\text{Fe}_{67}$  for the Ni-Fe nanotubes.

It has been reported by Brillson et al. (11) that if Ni diffuses into the surface of n-type InP, the Schottky barrier height decreases to about 0 eV, and thus is expected to behave as an ohmic contact. This suggests that the excellent piezoelectric properties may degenerate due to the formation of a Ni-P phase at the n-type InP / Ni-Fe interface, which might lead to the injection of free charge carriers into the InP pore walls. This problem can be easily overcome by covering the InP pore walls with a dielectric interlayer, e.g.

Si<sub>3</sub>N<sub>4</sub>, via atomic layer deposition (ALD). A positive side effect of this dielectric interlayer is that it should be possible to directly apply the Ni-Fe / Fe-Ga multilayer filling concept of Lupu et al. without encountering problems from the InP sidewalls.

### Conclusion and Outlook

The first steps on the way to a magnetoelectric composite sensor, which consists of a piezoelectric matrix material and a magnetostrictive filler material, have been made.

The fabrication of piezoelectric InP templates by electrochemical etching and additional purely post-etching in anorganic and organic acids has been demonstrated. The  $d_{14}$  component of macroporous InP is found to be around  $|60|$  pm/V, which is about a factor of 30 larger than the values reported for bulk InP. Though InP is the most suitable candidate for this approach in principle a new class of porous single-crystalline piezoelectric materials can be fabricated from III-V semiconductors by this process.

The galvanic filling of pores in InP with Ni-Fe is far from being trivial. It has been demonstrated that the galvanic filling with Ni-Fe is principally working, so that it seems possible to obtain completely filled pores even with high aspect ratios. The influence of the Ni-Fe / InP interface on the piezoelectric properties has to be investigated. By covering the InP pore walls with a dielectric interlayer, it should be possible to directly apply the Ni-Fe / Fe-Ga multilayer filling concept.

### Acknowledgements

This work was funded by the collaborative research center 855 “Magnetoelectric Composites – Future Biomagnetic Interfaces” by the DFG.

### References

1. J.F. Nye, *Physical properties of crystals: their representation by tensors and matrices*, Oxford University Press, Oxford (1985).
2. G. Arlt and P. Quadflieg, *Phys. Stat. Sol.* **25**, 323-330 (1968).
3. K. Rottner, R. Helbig, and G. Müller, *Appl. Phys. Lett.* **62(4)**, 352 (1993).
4. N. Lupu, H. Chiriac, and P. Pascariu, *J. Appl. Phys.* **103**, 07B511 (2008).
5. M. Leisner, J. Carstensen, and H. Föll, *Nanoscale Res. Lett.* **5(7)**, 1190 (2010).
6. S. Langa, I.M. Tiginyanu, J. Carstensen, M. Christophersen, and H. Föll, *Electrochem. Solid-State Lett.* **3(11)**, 514 (2000).
7. C.H. Lee, J.E. Bonevich, J.E. Davis, and T.P. Moffat, *J. Electrochem. Soc.* **155**, D499 (2008).
8. I. Tiginyanu, E. Monaico, and E. Monaico, *Electrochem. Comm.* **10(5)**, 731 (2008).
9. D. Kikuchi, Y. Matsui, and S. Adachi, *J. Electrochem. Soc.* **147(5)**, 1973 (2000).
10. H. Föll, H. Hartz, E.K. Ossei-Wusu, J. Carstensen, and O. Riemenschneider, *phys. stat. sol. RRL* **4(1)**, 4 (2010).
11. L.J. Brillson, C.F. Brucker, A.D. Katnani, N.G. Stoffel, and G. Margaritondo, *J. Appl. Phys. Lett.* **38**, 784 (1981).